



1 Controls of seasonality and altitude on generation of leaf water isotopes

2

3 Jinzhao Liu^{a, b*}, Huawu Wu^{c*}, Haiwei Zhang^d, Guoqiang Peng^e, Chong Jiang^a, Ying

4 Zhao^f, Jing Hu^a

5

6 ^a State Key Laboratory of Loess and Quaternary Geology, Institute of Earth Environment,

7 Chinese Academy of Sciences, Xi'an 710061, China

8 ^b CAS Center for Excellence in Quaternary Science and Global Change, Xi'an, 710061, China.

9 ^c Key Laboratory of Watershed Geographic Sciences, Nanjing Institute of Geography and
10 Limnology, Chinese Academy of Sciences, Nanjing 210008, China

11 ^d Institute of Global Environmental Change, Xi'an Jiaotong University, Xi'an, 710054, China

12 ^e School of Geography and Tourism, Shaanxi Normal University, Xi'an 710062, Shaanxi, China

13 ^f College of resources and environmental engineering, Ludong University, 264025, Yantai,
14 China

15

16 *Corresponding author's email: liujinzhao@ieecas.cn (J. Liu) and wuhuawu416@163.com (H.

17 Wu)

18

19

20

21

22



23 **Abstract**

24 Stable oxygen and hydrogen isotopes ($\delta^{18}\text{O}$ and $\delta^2\text{H}$) of leaf water which bridges
25 between hydrological processes and plant-derived organic materials vary spatially and
26 temporally. It is critical to study what controls the $\delta^{18}\text{O}$ and $\delta^2\text{H}$ values of leaf water for
27 a wide range of applications. Here, we repeatedly sampled soil water, stem water, and
28 leaf water along an elevation transect across seasons on the Chinese Loess Plateau and
29 analyzed the variations in the $\delta^{18}\text{O}$ and $\delta^2\text{H}$ values from precipitation, soil water, stem
30 water, and leaf water. We found consistency in the $\delta^{18}\text{O}$ and $\delta^2\text{H}$ values in precipitation,
31 soil water, stem water, and leaf water across seasons, indicating that leaf water can
32 record the isotopic signals of precipitation well. Importantly, leaf water isotope lines
33 were generated by the first-order control of source water (soil water and precipitation)
34 associated with seasonality and altitude, as well as the secondary control of
35 hydroclimate and biochemical factors resulting in weak correlations of the $\delta^{18}\text{O}$ and
36 $\delta^2\text{H}$ values in leaf water. This study improves our understanding of the generation of
37 leaf water isotopes.

38

39 **Short Summary**

40 Why do leaf water isotopes can generate to be an isotopic line in a dual-isotope plot?
41 This isotopic water line is as important as the local meteoric water line (LMWL) in the
42 isotope ecohydrology field. We analyzed the variations of oxygen and hydrogen
43 isotopes in soil water, stem water, and leaf water along an elevation transect across
44 seasons. We found that both seasonality and altitude affecting source water are likely



45 to result in the generation of an isotopic water line in leaf water.

46

47 Keywords: Leaf water, stable isotope, controls, seasonality, altitude

48

49 1 Introduction

50 The stable isotope compositions of water ($\delta^{18}\text{O}$ and $\delta^2\text{H}$) are increasingly used as
51 powerful tracers to follow the movement of water from its input as precipitation,
52 movement through the soil, and ultimately to its release as soil evaporation and leaf
53 transpiration (Mook, 2001; Penna and Meerveld, 2019). Leaf water transpiration plays
54 a key role in regulating the water balance at scales ranging from catchments to the globe.
55 Terrestrial plants can enrich heavier isotopes (^2H and ^{18}O) in leaf water due to
56 evapotranspiration (Helliker and Ehleinger, 2000; Liu et al., 2015; Cernusak et al.,
57 2016), which is highly dependent on atmospheric conditions (e.g., temperature and
58 relative humidity) and biophysiological processes (Farquhar et al., 2007; Kahmen et al.,
59 2011; Cernusak et al., 2016). Subsequently, the isotope signals of leaf water are
60 integrated into plant organic materials, such as cellulose (e.g., Barbour, 2007; Lehman
61 et al., 2017) and leaf wax (Liu et al., 2016, 2021) as powerful proxies used for
62 paleoclimate reconstruction (Pagani et al., 2006; Schefuß et al., 2011; Hepp et al.,
63 2020). Therefore, leaf water $\delta^{18}\text{O}$ and $\delta^2\text{H}$ values ($\delta^{18}\text{O}_{\text{lw}}$ and $\delta^2\text{H}_{\text{lw}}$) are the fundamental
64 parameters required for an in-depth understanding of these plant organic biomarkers in
65 paleoclimate contexts.

66



67 $\delta^{18}\text{O}_{\text{lw}}$ and $\delta^2\text{H}_{\text{lw}}$ values are influenced first by the plant's source water (mainly water
68 taken up by roots from the soil; Munksgaard et al., 2016; Cernusak et al., 2016). Soil
69 water for terrestrial plants generally originates from local precipitation, which serves as
70 a critical component of the water cycle. Precipitation isotopes vary spatially and
71 temporally, being subject to controls by the temperature, altitude, latitude, distance from
72 the coast, and amount of precipitation (Bowen, 2010; Bowen and Good, 2015; Cernusak
73 et al., 2016). Soil water isotopes are determined by a mixture of individual precipitation
74 events with distinct isotope signals and are also affected by evaporation, both of which
75 lead to isotopic gradients of soil water with depth (Allison et al., 1983; Liu et al., 2015).
76 A number of studies have shown that the $\delta^{18}\text{O}$ and $\delta^2\text{H}$ values of root/xylem water can
77 be used to characterize the water sources used by plants (Jia et al., 2013; Rothfuss and
78 Javaux, 2017; Wu et al., 2018; Wang et al., 2019; Amin et al., 2020; Zhao et al., 2020;
79 Liu et al., 2021a), and these studies rested on an assumption that no isotope
80 fractionations of $\delta^{18}\text{O}$ and $\delta^2\text{H}$ values occurred during water uptake by plant roots
81 (Dawson and Ehleringer, 1991; Ehleringer and Dawson, 1992; Chen et al., 2020),
82 except in saline or xeric environments (Lin and Sternberg, 1993; Ellsworth and
83 Williams, 2007). Some recent studies showed, however, that the occurrence of isotopic
84 fractionation during root water uptake was likely more common, especially regarding
85 the $\delta^2\text{H}$ values (Zhao et al., 2016; Wang et al., 2017; Barbeta et al., 2019; Poca et al.,
86 2019; Liu et al., 2021a). Therefore, studying the isotopic variations in the water
87 continuum from precipitation, soil water, stem water, to leaf water will help provide
88 substantial insight into understanding the spatiotemporal variations in leaf water



89 isotopes.

90

91 In addition to being influenced by plant source water, $\delta^{18}\text{O}_{\text{lw}}$ and $\delta^2\text{H}_{\text{lw}}$ values are
92 influenced by the evaporative process of transpiration and the isotopic composition of
93 the vapour in the atmosphere surrounding the leaf, the influences of which can be
94 predicted using the Craig-Gordon model (Craig and Gordon, 1965), which has been
95 modified for leaves under steady-state conditions (Dongmann et al., 1974; Farquhar et
96 al., 1989; Farquhar and Cernusak, 2005):

$$97 \quad \Delta_e = \varepsilon^+ + \varepsilon_k + (\Delta_v - \varepsilon_k) \frac{e_a}{e_i}$$

98 where Δ_e is the enrichment of evaporative site water above source water, ε^+ is the
99 equilibrium fractionation between liquid water and vapour, ε_k is the kinetic
100 fractionation during the diffusion of vapour through the stomata and the boundary layer,
101 Δ_v is the isotopic enrichment of vapour compared to source water, and $\left(\frac{e_a}{e_i}\right)$ is the ratio
102 of the water vapour pressure fraction in the air relative to that in the intercellular spaces,
103 which is equal to the relative humidity in the air. However, the model fails to explain
104 the intra-leaf heterogeneity of $\delta^{18}\text{O}_{\text{lw}}$ and $\delta^2\text{H}_{\text{lw}}$ (Cernusak et al., 2016; Liu et al., 2021b),
105 which is currently explained by a two-pool model (Leaney et al., 1985; Song et al.,
106 2015a) and/or an advection-diffusion model, as the *Péclet* effect (Farquhar and Lloyd,
107 1993; Farquhar and Gan, 2003). Subsequently, more complicated models under non-
108 steady-state conditions have been developed (Cuntz et al., 2007; Ogée et al., 2007).
109 These models emphasize on a mechanistic understanding of leaf water isotopic
110 fractionation, but under natural conditions, the relevant parameters cannot be strictly



111 constrained or precisely monitored which hinders the uses of these models (Plavcová
112 et al., 2018). Thus, the relationships between $\delta^{18}\text{O}_{\text{lw}}$ and/or $\delta^2\text{H}_{\text{lw}}$ and geo-climate
113 factors critically need to be resolved.

114

115 In this study, we measured the $\delta^{18}\text{O}_{\text{lw}}$ and $\delta^2\text{H}_{\text{lw}}$ values of precipitation, soil water, stem
116 water, and leaf water along an elevation transect across different seasons (i.e., spring,
117 summer, autumn). The objectives of our study were to better understand the seasonal
118 patterns of the leaf water $\delta^{18}\text{O}_{\text{lw}}$ and $\delta^2\text{H}_{\text{lw}}$ values, and the controls of altitude and
119 seasonality on the $\delta^{18}\text{O}_{\text{lw}}$ and $\delta^2\text{H}_{\text{lw}}$ values of leaf water generation. The results can help
120 to qualitatively and quantitatively evaluate the leaf water-based transpiration flux in
121 ecohydrological processes and the accuracy of plant organic biomarkers in natural
122 archives since they provide an insight into potential controls on leaf water isotopic
123 generation.

124

125 2 Materials and Methods

126 2.1 Study area

127 The Qinling Mountains form the dividing line between northern and southern China
128 and mark the boundary between the watersheds of the Yellow River and Yangtze River
129 valleys. Mt. Taibai (Fig. 1; 33. 96° N, 107.77° E; 3767 m asl) is the peak of the Qinling
130 Mountains, with a warm temperate ecosystem characterized by a rich and colourful
131 flora and fauna. The mean annual temperature at the bottom of Mt. Taibai is 12.9°C,
132 and the mean annual precipitation is 609.5 mm (Zhang and Liu, 2010). The climate,



133 soil, and vegetation vary significantly along the slope transect, exhibiting vertical geo-
134 ecological zonation (Fig. 1), which includes a variety of climate zones: warm temperate
135 (< 1300 m), temperate (1300 ~ 2600 m), cool temperate (2600 ~ 3350 m), and alpine (>
136 3350 m). The soil background covers yellow loess soil at low elevations, spectacular
137 rocky outcrops at middle elevations, and glacial remnants at high elevations; and the
138 vegetation consists mainly of coniferous and broadleaf forests, and alpine and subalpine
139 vegetation along the transect.

140 2.2 Sampling strategy

141 Plant and soil samples were performed in May, July and September 2020, and the
142 samples were collected from ten plots (3 × 3 m) along the northern slope of Mt. Taibai
143 extending from 608 m to 3533 m asl (Fig. 1). One or two plant species were
144 simultaneously collected; plant species were chose if they had a high abundance in the
145 community and/or were widely distributed for each plot. For plants, three stem and leaf
146 samples were collected for each species. Intact leaves with minimal damage were
147 collected from fully sunlit canopy branches considering the likely isotopic gradients
148 within a leaf (Liu et al., 2016). Suberized twigs were cut into 3-4 cm segments as a
149 sample, and these small plant segments were immediately placed into capped glass vials.
150 For soils, three surface soil samples (less than 10 cm) around the sampling plants were
151 taken using a small metal scoop. All sampled plots were located on slopes far away
152 from rivers and surface water bodies, which guaranteed that the soil water in each plot
153 was derived exclusively from precipitation. Although the surface soil layers were only
154 collected in this study, these samples provided a comparative reference for soil water



155 that originated from surface water instead of deep water, which is supported by a prior
156 study conducted at the same elevation transect (Zhang and Liu, 2010). The soil samples
157 were tightly sealed in a polyethylene zipper bag on site. All plant and soil samples were
158 frozen in a cooler ($\sim 4\text{ }^{\circ}\text{C}$) in the field and immediately transported to the laboratory.
159 The altitude of each plot was determined using a handheld GPS unit with an error of \pm
160 5 m.

161 2.3 Isotopic analyses

162 Water in plant and soil samples was extracted using an automatic cryogenic vacuum
163 extraction system (LI-2100 Pro, LICA United Technology Limited, Beijing, China).
164 The auto-extraction process was set for 3 hours, and the extraction rate of water from
165 samples was more than 98%. The isotopic composition of soil water was measured
166 using a Picarro L2130-I isotope water analyzer (Sunnyvale, CA, USA) at the State Key
167 Laboratory of Loess and Quaternary Geology, Institute of Earth Environment, Chinese
168 Academy of Science. The analytical accuracies were $\pm 0.1\text{‰}$ for $\delta^{18}\text{O}$ and $\pm 1\text{‰}$ for
169 $\delta^2\text{H}$. The isotopic measurements of root and leaf waters were conducted using an
170 isotope ratio mass spectrometer coupled with a high-temperature conversion elemental
171 analyzer (HT2000 EA-IRMS, Delta V Advantage; Thermo Fisher Scientific, Inc. USA)
172 in Huake Precision Stable Isotope Laboratory at the campus of Tsinghua University
173 Shenzhen International Graduation School. The measurement precisions were $\pm 0.2\text{‰}$
174 and $\pm 1\text{‰}$ for $\delta^{18}\text{O}$ and $\delta^2\text{H}$, respectively. The isotopic composition of $\delta^{18}\text{O}$ and $\delta^2\text{H}$ is
175 expressed as an isotope ratio:

$$176 \delta_{\text{sample}}(\text{‰}) = \left(\frac{R_{\text{sample}} - R_{\text{standard}}}{R_{\text{standard}}} \right) \times 1000 \quad (1)$$



177 where δ_{sample} represents $\delta^{18}\text{O}$ or $\delta^2\text{H}$, and R_{sample} and $R_{standard}$ indicate the ratio
178 of $^{18}\text{O}/^{16}\text{O}$ or $^2\text{H}/^1\text{H}$ of the sample and standard, respectively. The $\delta^{18}\text{O}$ and $\delta^2\text{H}$ values
179 are reported relative to the Vienna mean standard ocean water (VSMOW). The $\delta^{18}\text{O}$
180 and $\delta^2\text{H}$ values of precipitation were determined by the Online Isotope in Precipitation
181 Calculator (Bowen and Revenaugh, 2003).

182 2.4 Data analysis

183 Statistical analyses (e.g., mean, max., min., and s.d.) for isotopes of precipitation, soil,
184 stem and leaf waters were performed to show the range and distribution of $\delta^{18}\text{O}$ and
185 $\delta^2\text{H}$. Pearson correlation was conducted to describe the various correlations between
186 $\delta^{18}\text{O}$ and $\delta^2\text{H}$ among the different water types (e.g., precipitation, soil water, stem water,
187 and leaf water) because the isotopic data were normally distributed according to the
188 Kolmogorov-Smirnov (K-S) test. One-way ANOVA combined with a post hoc Tukey's
189 least significant difference (LSD) test was performed to identify the significant
190 differences in isotopic compositions of precipitation, soil, stem, and leaf waters across
191 months. Comparisons of the relationships of $\delta^{18}\text{O}$ and $\delta^2\text{H}$ for soil water and leaf water
192 were performed by using analysis of covariance (ANCOVA) to compare slopes across
193 months. The significance level for all statistical tests was set to the 95% confidence
194 interval. Moreover, the Hybrid Single-Particle Lagrangian Integrated Trajectory
195 (HYSPPLIT) model (Draxler and Rolph, 2003) was used to perform air mass back-
196 trajectory calculations for a central site (34.13°N, 107.83°E, 2270 m asl) of the study
197 area. Trajectories were initiated four times daily (at 00:00, 06:00, 12:00, and 18:00 UTC)
198 and their air parcel was released at 2300 m asl for May, July and September 2020 and



199 moved backward by winds for 120 h (5 days).

200

201 3 Results

202 3.1 Seasonal variations

203 The $\delta^{18}\text{O}$ and $\delta^2\text{H}$ values in precipitation, soil water, stem water, and leaf water varied
204 significantly among them across months (Fig. 2). The $\delta^{18}\text{O}$ values of precipitation, soil
205 water, stem water, and leaf water were $-7.7 \pm 2.0\text{‰}$, $-3.8 \pm 3.4\text{‰}$, $1.9 \pm 4.2\text{‰}$, and 4.7
206 $\pm 3.0\text{‰}$ in May, $-9.1 \pm 1.4\text{‰}$, $-11.5 \pm 1.3\text{‰}$, $3.4 \pm 2.6\text{‰}$, and $1.4 \pm 4.1\text{‰}$ in July, and -
207 $9.5 \pm 1.5\text{‰}$, $-11.6 \pm 1.3\text{‰}$, $7.5 \pm 6.7\text{‰}$, and $9.7 \pm 5.6\text{‰}$ in September, respectively.
208 Likewise, the $\delta^2\text{H}$ values of precipitation, soil water, stem water, and leaf water were -
209 $50.7 \pm 13.9\text{‰}$, $-47.1 \pm 10.5\text{‰}$, $-31.6 \pm 20.3\text{‰}$, and $-18.2 \pm 14.5\text{‰}$ in May, $-63.0 \pm 9.7\text{‰}$,
210 $-92.1 \pm 9.9\text{‰}$, $-69.9 \pm 15.2\text{‰}$, and $-54.4 \pm 12.8\text{‰}$ in July, and $-66.4 \pm 10.6\text{‰}$, $-87.7 \pm$
211 11.9‰ , $-84.5 \pm 25.2\text{‰}$, and $-97.0 \pm 28.0\text{‰}$ in September, respectively. Both the $\delta^{18}\text{O}$
212 and $\delta^2\text{H}$ values for all four water types (i.e., precipitation, soil water, stem water, and
213 leaf water) were significantly different ($p < 0.05$), exhibiting relatively heavier values
214 in May, intermediate values in July, and lower values in September, except for the $\delta^{18}\text{O}$
215 values in soil water (Fig. 2).

216 3.2 Correlations of $\delta^{18}\text{O}$ and $\delta^2\text{H}$ values

217 Significant correlations of the $\delta^{18}\text{O}$ and $\delta^2\text{H}$ values in different water types were
218 observed across months (Fig. 3). The local meteoric water lines (LMWLs) were
219 obtained from the $\delta^{18}\text{O}$ and $\delta^2\text{H}$ values of precipitation, in which of the slopes and
220 intercepts varied slightly across months (7.04, 6.79 and 6.85 for slopes and 3.26, -1.12



221 and -1.42 for intercepts in May, July and September, respectively). Similarly, the
222 regression lines of the $\delta^{18}\text{O}$ and $\delta^2\text{H}$ values from soil water, stem water, and leaf water
223 were observed (Fig. 3), suggesting that leaf water isotopes could well inherit the
224 isotopic signals of source waters that originated from stem water, soil water, and
225 ultimately precipitation. However, the slopes and coefficients of determination (R^2) of
226 the $\delta^{18}\text{O}$ and $\delta^2\text{H}$ values showed consistent decreasing trends from precipitation, soil
227 water, stem water and leaf water in all three months, except for soil water in May (Fig.
228 3). The ANCOVA tests showed no significant differences for the regression lines for
229 precipitation ($df = 0.47$, $F = 2.49$, $p = 0.11 > 0.05$), stem water ($df = 53.2$, $F = 0.42$, p
230 $= 0.66 > 0.05$), and leaf water ($df = 437.3$, $F = 2.78$, $p = 0.08 > 0.05$) across months,
231 but a significant difference for soil water across months ($df = 308.8$, $F = 10.9$, $p < 0.05$).
232 The difference in soil water regression lines across months was probably due to the
233 mixture of various precipitation events and evaporation in the upper soil layers (Yang
234 and Fu, 2017).

235 3.3 Altitude effects

236 Both the $\delta^{18}\text{O}$ and $\delta^2\text{H}$ values in precipitation and soil water decreased significantly
237 with an increase of altitude (Fig. 4; all for $R^2 > 0.37$, $p < 0.05$). Stem water and leaf
238 water showed decreasing trends for $\delta^2\text{H}$ in July ($R^2 = 0.82$ and 0.43) and for $\delta^{18}\text{O}$ (R^2
239 $= 0.61$ and 0.44) and $\delta^2\text{H}$ values ($R^2 = 0.84$ and 0.90) in September; in contrast, there
240 were nonsignificant correlations between isotopes in stem water and leaf water and
241 altitude for $\delta^{18}\text{O}$ values in July and for both $\delta^{18}\text{O}$ and $\delta^2\text{H}$ values in September (Fig. 4).

242



243 4 Discussion

244 4.1 Consistent variations among water types

245 We found a seasonal consistency in the $\delta^{18}\text{O}$ and $\delta^2\text{H}$ values from precipitation to soil
246 water, stem water, and ultimately leaf water (Fig. 2). This finding of temporal
247 consistency among water types (i.e., precipitation, soil water, stem water, leaf water)
248 has been observed in a number of studies (Phillips and Ehleringer, 1995; Cernusak et
249 al., 2005; Sprenger et al., 2016; Berry et al., 2017; Liu et al., 2021a). The isotopic
250 inheritance from precipitation to leaf water indicated that seasonal variations in the
251 precipitation $\delta^{18}\text{O}$ and $\delta^2\text{H}$ values could exert the first order of control on the temporal
252 patterns of leaf water. The spatiotemporal variability of the precipitation $\delta^{18}\text{O}$ and $\delta^2\text{H}$
253 values could be explained by a combination of effects such as temperature, altitude,
254 latitude, continent, and amount, which are associated with orographic conditions, sub-
255 cloud evaporation, moisture recycling, and differences in the vapor source at the
256 regional and continental scales (Dansgaard, 1964; McGuire and McDonnell, 2007; Li
257 et al., 2016; Penna and Meerveld, 2019; Wu et al., 2019). Our recent study, conducted
258 approximately 200 km away from the observed transect on the Chinese Loess Plateau,
259 demonstrated that the temperature effect (i.e., altitude effect), but not the precipitation
260 amount effect, was the dominant control on the precipitation $\delta^{18}\text{O}$ and $\delta^2\text{H}$ values (Liu
261 et al., 2021a). The underlying mechanism of the temperature effect in monsoon regions
262 is very complicated because three typical processes coexist: 1) the evaporation
263 condition over the vapour source area affects the initial isotopic ratio of atmospheric
264 moisture; 2) the transportation process of the water vapour affects the extent of rainfall



265 of the air mass during the course of transportation; and 3) the extent of condensation of
266 the vapour is influenced by the condensation temperature (Pang et al., 2006; Li et al.,
267 2019).

268

269 The $\delta^{18}\text{O}$ and $\delta^2\text{H}$ values from soil water, stem water and leaf water were isotopically
270 heavier in May, intermediate in July, and lowest in September, responding well to the
271 decreasing trends of precipitation $\delta^{18}\text{O}$ and $\delta^2\text{H}$ values (Fig. 2). The monthly variations
272 in precipitation $\delta^{18}\text{O}$ and $\delta^2\text{H}$ values from the Global Network for Isotopes in
273 Precipitation (GNIP, <http://www.iaea.org/>) at Xi'an station (1985-1992 AD), ca. 100
274 km away from our study transect, were ^{18}O - and ^2H -enriched in May relative to July
275 and September (Fig. 5a, b). The cluster mean of moisture transport routes using
276 HYSPLIT (Draxler and Rolph, 2003) and climatological 850 hPa wind vectors showed
277 that the main moisture was from western China and central Asia in May, from the
278 China-India Peninsula and the Bay of Bangle, and from the local moisture recycling
279 and convection (Fig. 5c, d, e). The seasonal variation of precipitation $\delta^{18}\text{O}$ and $\delta^2\text{H}$
280 values is consistently related to the onset, advancement and retreat of the Asian summer
281 monsoon and associated large-scale monsoon circulation change (e.g., Cheng et al.,
282 2009; Zhang et al., 2020, 2021). As the summer monsoon starts in mid-May, the rainfall
283 season starts in southern China, however, the study area is mainly controlled by the
284 moisture from westerlies (Chiang et al., 2015) with relatively higher
285 vapour/precipitation $\delta^{18}\text{O}$ and $\delta^2\text{H}$ values (Fig. 5c, a, b). In July, the summer monsoon
286 reaches its strongest phase, the rainfall belt shifts to central and northern China, and the



287 southerly wind brings plenty of moisture from the China-India Peninsula and the Bay
288 of Bangle with lower vapour/precipitation $\delta^{18}\text{O}$ and $\delta^2\text{H}$ values (Fig. 5d, a, b). When
289 the summer monsoon withdraws in September, the study area is mainly controlled by
290 moisture from local moisture recycling and convection (Fig. 5e). Soil water stores June-
291 August monsoon rainfall with lower $\delta^{18}\text{O}$ and $\delta^2\text{H}$ values, resulting in further lower
292 precipitation $\delta^{18}\text{O}$ and $\delta^2\text{H}$ values in September than those in July (Fig. 5a, b), and thus
293 resulting in significantly lower $\delta^{18}\text{O}_{\text{lw}}$ and $\delta^2\text{H}_{\text{lw}}$ values (Fig. 6).

294

295 4.2 Generation of leaf water isotope line

296 The LMWL, generated by the precipitation $\delta^{18}\text{O}$ and $\delta^2\text{H}$ values at the observed
297 locations (Fig. 2), is an important reference line for ecohydrological process and acts
298 as a benchmark for comparison among different water types. The LMWLs in May
299 (spring), July (summer) and September (autumn) were slightly smaller than the global
300 meteoric water line (GMWL: $\delta^2\text{H} = 8.17 \times \delta^{18}\text{O} + 10.35$; Rozanski et al., 2013),
301 suggesting different water vapour sources in the local circulation system and strong
302 evaporative fractionation under arid conditions. Across months, July precipitation
303 tended to have an isotopically lower slope value (6.79) than that of both May (7.04) and
304 September precipitation (6.85), but the difference across months was not significant (p
305 $= 0.11 > 0.05$). The slopes of the LMWLs from different months indicated that the water
306 vapour of precipitation across seasons came from the same source but suffered from
307 different intensities of evaporation due to temperature (Wu et al., 2019; Li et al., 2019).
308 Likewise, the regression lines of the $\delta^{18}\text{O}$ and $\delta^2\text{H}$ values in soil water, stem water, and



309 leaf water were observed across months (Fig. 3). The slopes in other water types (i.e.,
310 soil water, stem water, and leaf water) were relatively lower than the LMWLs, in which
311 the slopes for soil water and stem water were intermediates; however, they were lowest
312 for leaf water across seasons, except for soil water in May (Fig. 3). These observations
313 were supported by a variety of studies (Brooks et al., 2010; Evaristo et al., 2015;
314 Sprenger et al., 2016, 2017; Wang et al., 2017; Benettin et al., 2018; Barbeta et al., 2019;
315 Penna and Meerveld, 2019; Liu et al., 2021a) due to the occurrence of secondary
316 evaporation in other water types. Moreover, the R^2 values of dual-isotope space ($\delta^{18}\text{O}$
317 and $\delta^2\text{H}$) decrease significantly from precipitation, soil water, stem water and leaf water
318 in all seasons (Fig. 3), suggesting that besides physically evaporative fractionation,
319 other factors likely affect the $\delta^{18}\text{O}$ and $\delta^2\text{H}$ values in leaf water. Although the
320 abovementioned Craig-Gordon model has been used to explain the variation in $\delta^{18}\text{O}$
321 and $\delta^2\text{H}$ values in leaf water, the factors that control the leaf water $\delta^{18}\text{O}$ and $\delta^2\text{H}$ values
322 under non-steady-state conditions and the *Péclet* effect remain to be further studied
323 (Song et al., 2015b; Cernusak et al., 2016; Barbour et al., 2017).

324 In a dual-isotope space in leaf water, a significantly distributed pattern across months
325 was observed: isotopically depleted in September, intermediate in July, and enriched in
326 May (Fig. 6). When focusing on each month, we found relatively higher isotopic values
327 occurring at low elevations but lower isotopic values at high elevations despite no or
328 weak correlations between altitude and $\delta^{18}\text{O}/\delta^2\text{H}$ values (Fig. 4). Combining these two
329 effects (i.e., seasonality and altitude), the $\delta^{18}\text{O}$ and $\delta^2\text{H}$ values in leaf water yield a
330 remarkable isotopic line in the dual-isotope plot (Fig. 3), which typically lies at the right



331 of the LMWLs. This result is supported by a recent study that conducted consecutive
332 measurements of $\delta^{18}\text{O}$ and $\delta^2\text{H}$ values in xylem/leaf water in Switzerland and indicated
333 that leaf water provides great potential to determine source water of plants (Benettin et
334 al., 2021). A schematic of effects of seasonality and altitude on leaf water $\delta^{18}\text{O}$ and $\delta^2\text{H}$
335 values is shown in Fig. 7, which involves many of hydroclimatic and biochemical
336 factors that control the leaf water $\delta^{18}\text{O}$ and $\delta^2\text{H}$ values. Significant isotopic fractionation
337 occurred mainly at two key locations across vertical soil profiles and leaf architectures
338 from precipitation to leaf water, but both seasonality and altitude, in essence, affected
339 the precipitation $\delta^{18}\text{O}$ and $\delta^2\text{H}$ values (Fig. 7). An isotopic gradient across the vertical
340 soil profile appeared because of evaporation at the surface soil layers (Ehleringer et al.,
341 1992; Goldsmith et al., 2012; Evaristo et al., 2015), which led to a linear enrichment
342 trajectory in the soil water dual-isotope plot (Goldsmith et al., 2012; Jia et al., 2013;
343 Rothfuss and Javaux, 2017; Wu et al., 2018; Wang et al., 2019; Amin et al., 2020; Zhao
344 et al., 2020; Liu et al., 2021a). The soil water isotope line provides a water source for
345 leaf water isotope line generation. However, biochemical factors also exert an effect on
346 leaf water $\delta^{18}\text{O}$ and $\delta^2\text{H}$ values, as supported by different $\delta^2\text{H}$ enrichments in leaf water
347 between dicots and monocots, associated with leaf veinal structures (Liu et al., 2021b).
348 This result is consistent with the weaker correlations of $\delta^{18}\text{O}$ and $\delta^2\text{H}$ values in leaf
349 water than in soil water (Fig. 3). Collectively, the leaf water isotope line is generated
350 by the first-order control of spatiotemporal variation in the precipitation $\delta^{18}\text{O}$ and $\delta^2\text{H}$
351 values (associated with seasonality and altitude) and secondarily affected by
352 biochemical factors within a leaf.



353

354 4.3 Insights and implications

355 The ecohydrological cycle over continents primarily involves the input from
356 precipitation and the output to the atmosphere through evapotranspiration. Among them,
357 leaf water transpiration is a key component of water cycle in terrestrial ecosystems.
358 Stable isotope technique of leaf water has been used to estimate transpiration through
359 leaf surface, contributing up to 50 to 90% of ecosystem evapotranspiration (Jasechko
360 et al., 2013; Schlesinger and Jasechko, 2014). Moreover, the $\delta^{18}\text{O}$ values of leaf water
361 partly influences the oxygen isotope values of atmospheric CO_2 (Farquhar et al., 1993),
362 which can be helpful to constrain global carbon cycle. All of these various applications
363 rest on a firm understanding of the mechanisms that control leaf water $\delta^{18}\text{O}$ and $\delta^2\text{H}$
364 values (Cernusak et al., 2016).

365

366 However, there were great variabilities in leaf water $\delta^{18}\text{O}$ and $\delta^2\text{H}$ values over diurnal
367 and seasonal cycle. For example, leaf water $\delta^{18}\text{O}$ and $\delta^2\text{H}$ values generally showed a
368 maximum in the early afternoon and a minimum in the early morning (Cernusak et al.,
369 2016). Our results showed a seasonal variation in leaf water $\delta^{18}\text{O}$ and $\delta^2\text{H}$ values, which
370 followed the isotopic patterns in other waters such as stem water, soil water and
371 precipitation. The seasonal variability in leaf water $\delta^{18}\text{O}$ and $\delta^2\text{H}$ values has also been
372 observed in tropical monsoon condition (Hartsough et al., 2008). The diurnal and
373 seasonal variations in leaf water $\delta^{18}\text{O}$ and $\delta^2\text{H}$ values indicate the leaf water isotopic
374 line would vary with time. Moreover, as we all known, the LMWL varies significantly



375 over space, with the slopes ranging between 5 and 6.5 in middle latitudes and between
376 2 and 5 in arid climates (Gibson et al., 2008; Sprenger et al., 2016). Collectively, the
377 leaf water isotope line will vary temporally and spatially. Thus, it needs to be widely
378 explored for the spatio-temporal variations of leaf water isotope line in the future
379 studies.

380

381 5 Conclusion

382 Along the elevation transect, precipitation, soil water, stem water, and leaf water were
383 repeatedly sampled to analyze for $\delta^{18}\text{O}$ and $\delta^2\text{H}$ values associated with season and
384 altitude. There was a seasonal consistency of $\delta^{18}\text{O}$ and $\delta^2\text{H}$ values from precipitation,
385 soil water, stem water, and ultimate leaf water, suggesting that leaf water recorded well
386 the isotopic signals of precipitation, which was primarily affected by the water vapour
387 source in our studied transect. Moreover, both $\delta^{18}\text{O}$ and $\delta^2\text{H}$ values of precipitation and
388 soil water were significantly correlated with altitude, but no or weak correlations
389 occurred between $\delta^{18}\text{O}$ and $\delta^2\text{H}$ values of stem/leaf water and altitude, which indicated
390 that besides source water (i.e., precipitation, soil water), biochemical factors likely
391 exerted a secondary control on leaf water $\delta^{18}\text{O}$ and $\delta^2\text{H}$ values. Therefore, leaf water
392 isotopes were controlled by combined effects of source water and leaf water
393 transpiration surrounding the leaf surface, in which seasonality and altitude acted as a
394 trigger to form a leaf water isotopic line.

395

396 **Data availability statement**



397 Data related to this article can be found in Electric Annex and Mendeley Data
398 (<https://data.mendeley.com/drafts/t44wybgpr3>).

399

400 **Author contribution**

401 J.L. conceived the idea of research. J.L. and H.W. performed the data analysis and wrote
402 the manuscript. H.W. and H.Z. edited the paper. C.J. and J.H. performed the lab work.
403 All authors contributed to discuss the results.

404

405 **Competing interests**

406 The authors declare that they have no known competing financial interests or
407 personal relationships that could have appeared to influence the work reported in this
408 paper.

409

410 **Acknowledgement**

411 We would like to thank X. Cao and M. Xing for their help with laboratory assistance
412 and Y. Cheng for helps in the field. We thank Prof. J. J. McDonnell for pre-discussing
413 the framework of the paper. This work was supported by the Chinese Academy of
414 Sciences (XAB2019B02; ZDBS-LY-DQC033) and National Natural Science
415 Foundation of China (42073017), and by the open fund from State Key Laboratory of
416 Loess and Quaternary Geology (SKLLQG1926).

417

418 **References**



- 419 Amin, A., Zuecco, G., Geris, J., Schwendenmann, L., McDonnell, J.J., Borga, M.,
420 Penna, D., 2020. Depth distribution of soil water sourced by plants at the global scale:
421 a new direct inference approach. *Ecohydrology* 13, e2177.
- 422 Allison, G., Barnes, C., and Hughes, M., 1983. The distribution of deuterium and ^{18}O
423 in dry soils 2. *Experimental, J. Hydrol.* 64, 377–397.
- 424 Barbata A, Jones SP, Clavé L, Gimeno TE, Fréjaville B, Wohl S, Ogée J, 2019.
425 Unexplained hydrogen isotope offsets complicate the identification and quantification
426 of tree water sources in a riparian forest. *Hydrol Earth Syst Sci* 23, 2129-2146.
- 427 Barbour, M.M., 2007. Stable oxygen isotope composition of plant tissue: a review.
428 *Funct. Plant Biol.* 34, 83–94.
- 429 Barbour MM, Farquhar GD, Buckley TN, 2017. Leaf water stable isotopes and water
430 transport outside the xylem. *Plant Cell and Environment* 40, 914-920.
- 431 Benettin P, Nehemy MF, Cernusak LA, Kahmen A, McDonnell JJ, 2021. On the use of
432 leaf water to determine plant water source: A proof of concept. *Hydrological Processes*
433 DOI: 10.1002/hyp.14073
- 434 Benettin P., Volkman THM, von Freyberg J, Frentress J, Penna D, Dawson TE,
435 Kirchner JW, 2018. Effects of climatic seasonality on the isotopic composition of
436 evaporating soil waters. *Hydrol. Earth Syst. Sci.* 22, 2881-2890.
- 437 Berry, Z.C., Evaristo, J., Moore, G., Poca, M., Steppe, K., Verrot, L., Asbjornsen, H.,
438 Borma, L.S., Bretfeld, M., Herve-Fernandez, P., Seyfried, M., Schwendenmann, L.,
439 Sinacore, K., Wispelaere, L.D., McDonnell, J., 2017. The two water worlds hypothesis:
440 addressing multiple working hypotheses and proposing a way forward. *Ecohydrology*,



441 e1843.

442 Becker, A., Finger, P., Meyer-Christoffer, A., Rudolf, B., Ziese, M., 2011. GPCC full
443 data reanalysis version 6.0 at 1.0: monthly land-surface precipitation from rain-gauges
444 built on GTS-based and historic data. Global Precipitation Climatology Centre (GPCC):
445 Berlin, Germany.

446 Bowen, G.J., Revenaugh, J., 2003. Interpolating the isotopic composition of modern
447 meteoric precipitation. *Water Resour. Res.* 39, 1299.

448 Bowen, G. J. (2010). Isoscapes: Spatial pattern in isotopic biogeochemistry. *Annual*
449 *Review of Earth and Planetary Sciences*, 2010, 161–187.

450 Bowen GJ, Good SP, 2015. Incorporating water isoscapes in hydrological and water
451 resource investigations. *Wiley Interdiscip. Rev. Water* 2, 107–119.

452 Brooks JR, Barnard HR, Coulombe R, McDonnell JJ, 2010. Ecohydrologic separation
453 of water between trees and streams in a Mediterranean climate. *Nature Geoscience* 3,
454 100-104.

455 Cernusak, L.A., Farquhar, G.D., Pate, J.S., 2005. Environmental and physiological
456 controls over oxygen and carbon isotope composition of Tasmanian blue gum,
457 *Eucalyptus globulus*. *Tree Physiol.* 25, 129–146.

458 Cernusak LA, Barbour MM, Arndt SK, Cheesman AW, English NB, Feild TS, Helliker
459 BR, Holloway-Phillips MM, Holtum JAM, Kahmen A, McInerney FA, Munksgaard
460 NC, Simonin KA, Song X, Stuart-Williams H, West JB, Farquhar GD, 2016. Stable
461 isotopes in leaf water of terrestrial plants. *Plant Cell Environment* 39, 1087-1102.

462 Chen Y, Helliker BR, Tang X, Li F, Zhou Y, Song X, 2020. Stem water cryogenic



463 extraction biases estimation in deuterium isotope composition of plant source water.
464 Proceedings of the National Academy of the Sciences USA 117, 33345-33350.
465 Cheng, H., Sinha, A., Wang, X., Cruz, F.W., Edwards, R.L., 2012. The Global
466 Paleomonsoon as seen through speleothem records from Asia and the Americas.
467 Climate Dynamics 39, 1045-1062.
468 Chiang, J.C., Fung, I.Y., Wu, C.-H., Cai, Y., Edman, J.P., Liu, Y., Day, J.A.,
469 Bhattacharya, T., Mondal, Y., Labrousse, C.A., 2015. Role of seasonal transitions and
470 westerly jets in East Asian paleoclimate. Quaternary Science Reviews 108, 111-129.
471 Craig, H., Gordon, L.I., 1965. Deuterium and oxygen-18 variations in the ocean and
472 the marine atmosphere. In 'Proceedings of a conference on stable isotopes in
473 oceanographic studies and paleotemperatures'. pp. 9–130.
474 Dansgaard, W., 1964. Stable isotopes in precipitation. Tellus 16, 436–468.
475 Dawson, T. E. and Ehleringer, J. R., 1991. Streamside trees that do not use stream water,
476 Nature, 350, 335–337.
477 Dongmann G, Nurnberg HE, Forstel H, Wagener K (1974) On the enrichment of H₂¹⁸O
478 in the leaves of transpiring plants. Radiation and Environmental Biophysics **11**, 41–52.
479 Draxler, R.R., Rolph, G.D., 2003. HYSPLIT (Hybrid Single-Particle Lagrangian
480 Integrated Trajectory) Model Access via NOAA ARLREADY. htmlNOAA Air
481 Resources Laboratory. Website. <http://www.arl.noaa.gov/ready/hysplit4>.
482 Ehleringer, J. R. & Dawson, T. E. (1992) Water uptake by plants: perspectives from
483 stable isotope composition. *Plant Cell Environ.* **15**, 1073–1082.
484 Ehleringer, J. R. and Dawson, T. E., 1992. Water uptake by plants: perspectives from



485 stable isotope composition, *Plant Cell Environ.*, 15, 1073–1082,
486 Ellsowrth, P.Z., Williams, D.G., 2007. Hydrogen isotope fractionation during water
487 uptake by woody xerophytes. *Plant Soil* 291, 93–107.
488 Evaristo J., Jasechko S., McDonnell J.J. 2015. Global separation of plant transpiration
489 from groundwater and streamflow. *Nature* **525** : 91-94.
490 Farquhar, G.D., Cernusak, L.A., Barnes, B., 2007. Heavy water fractionation during
491 transpiration. *Plant Physiol.* 143, 11–18.
492 Farquhar GD, Cernusak LA (2005) On the isotopic composition of leaf water in the
493 non- steady state. *Functional Plant Biology* **32**, 293–303.
494 Farquhar G.D., Gan K.S. (2003) On the progressive enrichment of the oxygen isotopic
495 composition of water along leaves. *Plant, Cell and Environment* 26, 801–819.
496 Farquhar G.D., Lloyd J. (1993) Carbon and oxygen isotope effects in the exchange of
497 carbon dioxide between terrestrial plants and the atmosphere. In *Stable Isotopes and*
498 *Plant Carbon–Water Relations* (eds J.R. Ehleringer, A.E. Hall, & G.D. Farquhar), pp.
499 47–70. Academic Press, San Diego.
500 Gibson JJ, Birks SJ, Edwards TWD, 2008. Global prediction of δA and $\delta^2H-\delta^{18}O$
501 evaporation slopes for lakes and soil water accounting for seasonality. *Global*
502 *Biogeochem. Cycles*, 22, GB2031
503 Goldsmith, G.R., Munoz-Villers, L.E., Holwerda, F., McDonnell, J.J., Asbjornsen, H.,
504 Dawson, T.E., 2012. Stable isotopes reveal linkages among ecohydrological processes
505 in a seasonally dry tropical montane cloud forest. *Ecohydrology* 5, 779–790.
506 Hartsough P, Poulson SR, Biondi F, Estrada IG, 2008. Stable isotope characterization



507 of the ecohydrological cycle at a tropical treeline site. Arctic, Antarctic, and Alpine
508 Research 40, 343-354.

509 Helliker, B.R., Ehleringer, J.R., 2000. Establishing a grassland signature in veins: ^{18}O
510 in the leaf water of C_3 and C_4 grasses. Proc. Natl. Acad. Sci. U.S.A. 97, 7894–7898.

511 Hepp J, Schäfer IK, Lanny V, Franke J, Blidner M, Rozanski K, Glaser B, Zech M,
512 Eglinton TI, Zech R, 2020. Evaluation of bacterial glycerol dialkyl glycerol tetraether
513 and ^2H - ^{18}O biomarker proxies along a central European topsoil transect.
514 Biogeosciences 17, 741-756.

515 Jasechko S, Sharp ZD, Gibson JJ, Birks SJ, Yi Y, Fawcett PJ, 2013. Terrestrial water
516 fluxes dominated by transpiration. Nature 496, 347-350.

517 Jia, X., Wang, Y., Shao, M., Luo, Y., Zhang, C., 2017. Estimating regional losses of soil
518 water due to the conversion of agricultural land to forest in China's Loess Plateau.
519 Ecohydrology 10, e1851.

520 Kahmen A., Sachse D., Arndt S.K., Tu K.P., Farrington H., Vitousek P.M. & Dawson
521 T.E. (2011) Cellulose $\delta^{18}\text{O}$ is an index of leaf-to-air vapor pressure difference (VPD) in
522 tropical plants. Proceedings of the National Academy of Sciences of the United States
523 of America, 108, 1981-1986.

524 Leaney F., Osmond C., Allison G. & Ziegler H. (1985) Hydrogen-isotope composition
525 of leaf water in C_3 and C_4 plants: its relationship to the hydrogen-isotope composition
526 of dry matter. Planta 164, 215–220.

527 Lehmann, M. M., Gamarra, B., Kahmen, A., Siegwolf, R. T. W., & Saurer, M. (2017).
528 Oxygen isotope fractionations across individual leaf carbohydrates in grass and tree



- 529 species. *Plant, Cell & Environment* 40, 1658–1670.
- 530 Li Z, Feng Q, Wang Q, Kong Y, Cheng A, Yong S, Li Y, Li J, Guo X, 2016.
- 531 Contributions of local terrestrial evaporation and transpiration to precipitation using
- 532 $\delta^{18}\text{O}$ and D-excess as a proxy in Shiyang inland river basin in China. *Global and*
- 533 *Planetary Change* 146, 140-151.
- 534 Li Z, Li Z, Yu H, Song L, Ma J, 2019. Environmental significance and zonal
- 535 characteristics of stable isotope of atmospheric precipitation in arid Central Asia.
- 536 *Atmospheric Research* 227, 24-40.
- 537 Lin, G.H., Sternberg, L.S.L., 1993. Hydrogen isotopic fractionation by plant roots
- 538 during water uptake in coastal wetland plants. *Stable Isotopic and Plant Carbon/Water*
- 539 *Relations*. Academic Press, New York, pp. 497–510.
- 540 Liu, J., Liu, W., An, Z., 2015. Insight into the reasons of leaf wax $\delta\text{D}_{\text{n-alkane}}$ values
- 541 between grasses and woods. *Sci. Bull.* 60, 549–555.
- 542 Liu, J., Liu, W., An, Z., Yang, H., 2016. Different hydrogen isotope fractionations
- 543 during lipid formation in higher plants: Implications for paleohydrology. *Sci. Report* 6,
- 544 19711.
- 545 Liu J, Wu H, Cheng Y, Jin Z, Hu J, 2021a. Stable isotope analysis of soil and plant water
- 546 in a pair of natural grassland and understory of planted forestland on the Chinese Loess
- 547 Plateau. *Agricultural Water Management* 249, 106800.
- 548 Liu J, An Z, Lin G, 2021b. Intra-leaf heterogeneities of hydrogen isotope compositions
- 549 in leaf water and leaf wax of monocots and dicots. *Science of the Total Environment*
- 550 770, 145258.



- 551 McGuire, K., and J. McDonnell (2007), Stable isotope tracers in watershed hydrology,
552 in *Stable Isotopes in Ecology and Environmental Science, Ecological Methods and*
553 *Concepts Series*, pp. 334–374.
- 554 Munksgaard NC, Cheesman AW, English NB, Zwart C, Kahmen A, Cernusak LA, 2016.
555 Identifying drivers of leaf water and cellulose stable isotope enrichment in Eucalyptus
556 in northern Australia. *Oecologia* 183, 31-43.
- 557 Pang, H., He, Y., Lu, A., Zhao, J., Ning, B., Yuan, L., Song, B., 2006. Synoptic-scale
558 variation of $\delta^{18}\text{O}$ in summer monsoon rainfall at Lijiang, China. *Chin. Sci. Bull.* 51,
559 2897–2904.
- 560 Pagani M, Pedentchouk N, Huber M, Sluijs A, Schouten S, Brinkhuis H, Damsté J S S.
561 Dichens GR, 2006. Arctic hydrology during global warming at the Palaeocene/Eocene
562 thermal maximum. *Nature* 442, 671–675.
- 563 Penna D, van Meerveld HJ, 2019. Spatial variability in the isotopic composition of
564 water in small catchments and its effect on hydrograph separation. *WIREs Water*, e1367.
- 565 Phillips, S.L., Ehleringer, J.R., 1995. Limited uptake of summer precipitation by big
566 tooth maple (*Acer grandidentatum* Nutt) and Gambels oak (*Quercus gambelii* Nutt).
567 *Trees* 9, 214–219.
- 568 Plavcová L, Hronková M, Šimková M, Květoň J, Vráblová M, Kubásek J, Šantrůček J,
569 2018. Seasonal variation of $\delta^{18}\text{O}$ and $\delta^2\text{H}$ in leaf water of *Fagus sylvatica* L. and related
570 water compartments. *Journal of Plant Physiology* 227, 56-65.
- 571 Poca M, Coomans O, Urcelay C, Zeballos SR, Bodé S, Boecks P, 2019. Isotope
572 fractionation during root water uptake by *Acacia caven* is enhanced by arbuscular



573 mycorrhizas. *Plant and Soil*, 3.

574 Rienecker, M.M., Suarez, M.J., Gelaro, R., Todling, R., Bacmeister, J., Liu, E.,
575 Bosilovich, M.G., Schubert, S.D., Takacs, L., Kim, G.-K., 2011. MERRA: NASA's
576 modern-era retrospective analysis for research and applications. *Journal of Climate* 24,
577 3624-3648.

578 Rothfuss, Y., Javaux, M., 2017. Reviews and syntheses: isotopic approaches to quantify
579 root water uptake: a review and comparison of methods. *Biogeosciences* 14, 2199–2224.

580 Rozanski, K., Araguas-Araguas, L., Gonfiantini, R., 2013. Isotopic patterns in modern
581 global precipitation. *Geophys. Monogr. Ser.* 1–36.

582 Song X., Loucos K.E., Simonin K.A., Farquhar G.D., Barbour M.M., 2015a.
583 Measurements of transpiration isotopologues and leaf water to assess enrichment
584 models in cotton. *New Phytologist* 206, 637–646.

585 Song X, Simonin KA, Loucos KE, Barbour MM, 2015b. Modelling non-steady-state
586 isotope enrichment of leaf water in a gas-exchange cuvette environment. *Plant, Cell
587 and Environment* 38, 2618-2628.

588 Schefuß, E., Kuhlmann, H., Mollenhauer, G., Prange, M., Pätzold, J., 2011. Forcing of
589 wet phases in Southeast Africa over the past 17,000 year. *Nature* 480, 22–29.

590 Schleinger WH, Jasechko S, 2014. Transpiration in the global water cycle. *Agr. Forest
591 Meteorol.* 189-190, 115-117.

592 Sprenger M, Leistert H, Gimbel K, Weiler M, 2016. Illuminating hydrological
593 processes at the soil-vegetation-atmosphere interface with water stable isotopes. *Rev.
594 Geophys.* 54, 674-704.



- 595 Sprenger M, Tetzlaff D., Soulsby S., 2017. Soil water stable isotopes reveal evaporation
596 dynamics at the soil-plant-atmosphere interface of the critical zone. *Hydrol. Earth Syst.*
597 *Sci.* 21, 3839-3858.
- 598 Wang J, Fu B, Lu N, Zhang L, 2017. Seasonal variation in water uptake patterns of
599 three plant species based on stable isotopes in the semi-arid Loess Plateau. *Science of*
600 *the Total Environment* 609, 27-37.
- 601 Wang, J., Lu, N., Fu, B., 2019b. Inter-comparison of stable isotope mixing models for
602 determining plant water source partitioning. *Sci. Total Environ.* 666, 685–693.
- 603 Wu, H., Li, J., Li, X., He, B., Liu, J., Jiang, Z., Zhang, C., 2018. Contrasting response
604 of coexisting plant's water-use patterns to experimental precipitation manipulation in
605 an alpine grassland community of Qinghai Lake watershed, China. *PLoS One* 13,
606 e0194242.
- 607 Wu H, Wu J, Sakiev K, Liu J, Li J, He B, Liu Y, Shen B, 2019. Spatial and temporal
608 variability of stable isotopes ($\delta^{18}\text{O}$ and $\delta^2\text{H}$) in surface waters of arid, mountainous
609 Central Asia. *Hydrological Processes* 33, 1658-1669.
- 610 Yang, Y.G., Fu, B.J., 2017. Soil water migration in the unsaturated zone of semiarid
611 region in China from isotope evidence. *Hydrol. Earth Syst. Sci.* 21, 1–24.
- 612 Zhang P, Liu W, 2010. Effect of plant life form on relationship between δD values of
613 leaf wax n-alkanes and altitude along Mount Taibai, China. *Organic Geochemistry* 42,
614 100-107.
- 615 Zhao L, Wang L, Cernusak LA, Liu X, Xiao H, Zhou M, Zhang S, 2016. Significant
616 difference in hydrogen isotope composition between xylem and tissue water in *Populus*



617 *Euphratica*. Plant Cell Environ 39, 1848-1857.

618 Zhao, Y., Wang, Y., He, M., Tong, Y., Zhou, J., Guo, X., Liu, J., Zhang, X., 2020.

619 Transference of *Robinia pseudoacacia* water-use patterns from deep to shallow soil

620 layers during the transition period between the dry and rainy seasons in a waterlimited

621 region. For. Ecol. Manag. 457, 117727.

622 Zhang, H., Cheng, H., Cai, Y., Spötl, C., Sinha, A., Kathayat, G., Li, H., 2020. Effect of

623 precipitation seasonality on annual oxygen isotopic composition in the area of spring

624 persistent rain in southeastern China and its paleoclimatic implication. Climate of the

625 Past 16, 211-225.

626 Zhang, H., Zhang, X., Cai, Y., Sinha, A., Spötl, C., Baker, J., Kathayat, G., Liu, Z., Tian,

627 Y., Lu, J., 2021. A data-model comparison pinpoints Holocene spatiotemporal pattern

628 of East Asian summer monsoon. Quaternary Science Reviews 261, 106911.

629

630

631

631 **Figure captions**

632 Fig. 1 Sample sites (black dots) and vertical distribution of vegetation across the Mt. Taibai transect

633 (originating from Liu, 2021).

634 Fig. 2 Boxplots of precipitation, soil water, stem water, and leaf water for $\delta^{18}\text{O}$ values (a-d) and $\delta^2\text{H}$

635 values (e-h). Box plots show the median (red line), interquartile range (IQR) with the upper (75%)

636 and lower (25%) quartiles, lowest whisker still within 1.5 IQR of the lower quartile, and highest

637 whisker still within 1.5 IQR of the upper quartile; dots mark outliers.

638 Fig. 3 Dual isotope plots of precipitation, soil water, stem water, and leaf water in May (a), July (b),

639 and September (c).

640 Fig. 4 Relationships between altitude and $\delta^{18}\text{O}$ (a-c) and $\delta^2\text{H}$ values (d-f) from different water types

641 across months.

642 Fig. 5 Variation of monthly mean precipitation $\delta^{18}\text{O}$ (a) and $\delta^2\text{H}$ (b) values at Xi'an station from

643 Global Network of Isotopes in Precipitation (GNIP) and cluster mean of moisture transport routes

644 using HYSPLIT model in May (c), July (d) and September (e), 2020. Background in (c-e) is the

645 average precipitation (mm/day) and 850 hPa wind vectors (arrows, m/s) in May (c), July (d) and

646 September (e) in 1979-2016 AD based on the database of the Global Precipitation Climatology

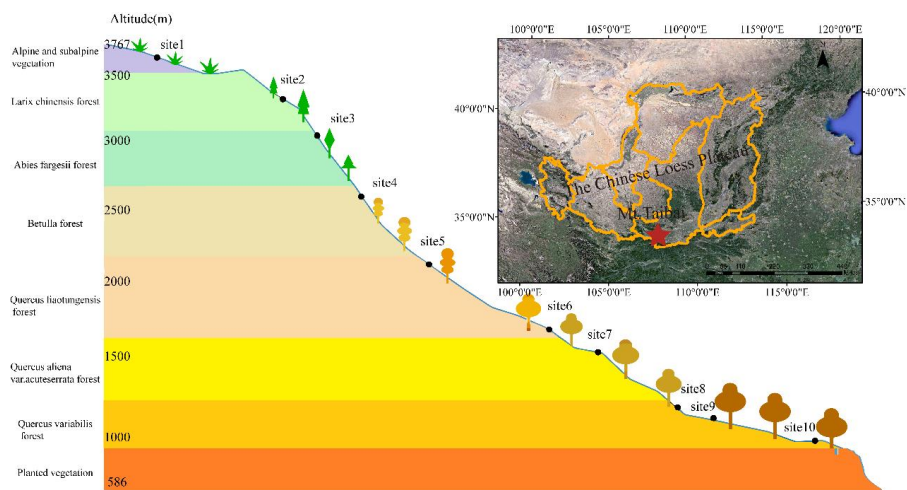


647 Center (GPCC) (Becker et al., 2011) and the Modern-Era Retrospective analysis for Research and
648 Applications (Rienecker et al., 2011).

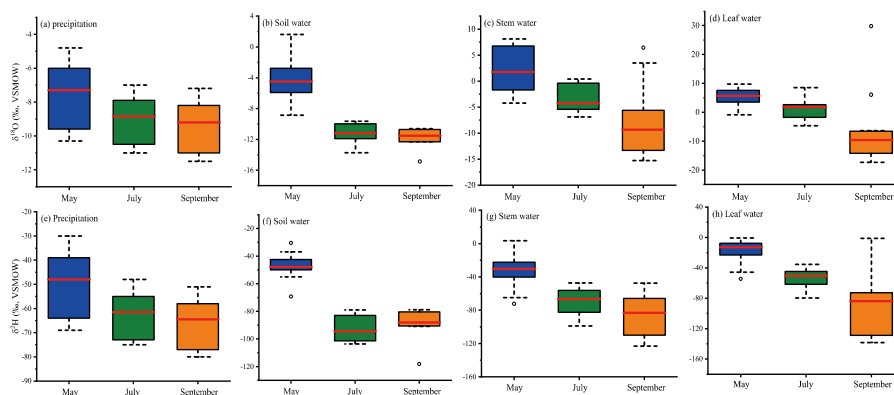
649 Fig. 6 Dual isotope plots for leaf water across month and altitude.

650 Fig. 7 Isotopic schematics of the flow diagram from precipitation to leaf water. Overview of the
651 processes through multiple isotopic fractionations associated with various hydroclimate and physio-
652 biological factors in terrestrial plants (Modified from Sachse et al., 2012 and Liu et al., 2016).

653
654
655
656
657
658
659
660
661
662
663
664
665
666
667
668

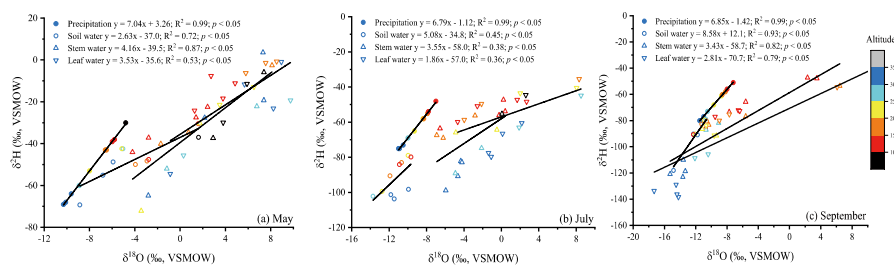


669
670 Figure-1
671
672



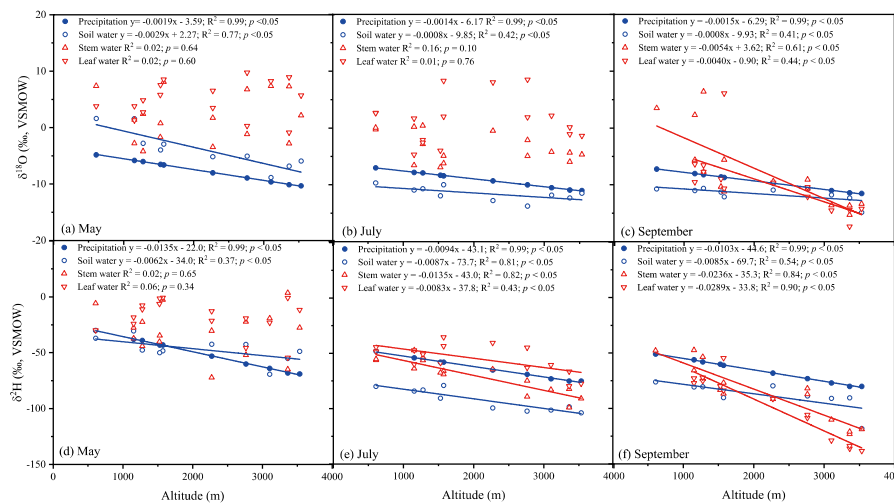
673
 674
 675
 676

Figure-2



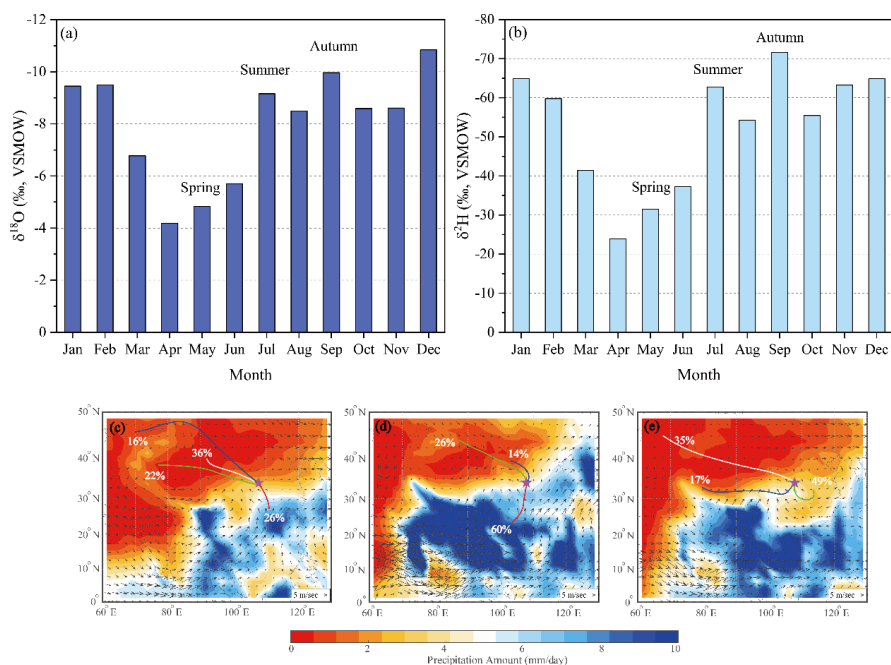
677
 678
 679
 680

Figure-3



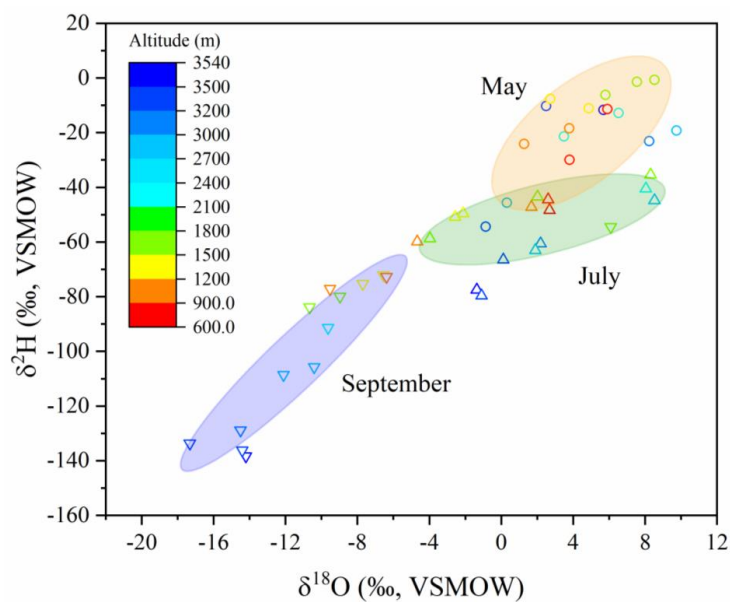
681
 682
 683
 684

Figure-4



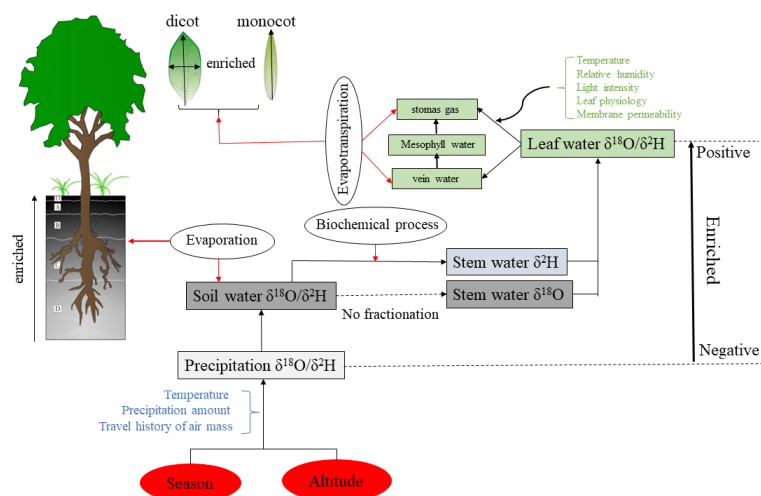
685
 686
 687
 688

Figure-5



689
 690
 691
 692

Figure-6



693

694 Figure-7

695

696